Microfluorimetric Analysis of a Purinergic Receptor ($P2X_7$) in GH_4C_1 Rat Pituitary Cells: Effects of a Bioactive Substance Produced by *Pfiesteria piscicida*

Ana Clara Melo,[1] Peter D.R. Moeller,[1] Howard Glasgow,[2] JoAnn M. Burkholder,[2] and John S. Ramsdell[1]

[1]Marine Biotoxins Program, Center for Coastal Environmental Health and Biomolecular Research, National Oceanic & Atmospheric Administration-National Ocean Service, Charleston, South Carolina, USA; [2]Department of Botany, North Carolina State University, Raleigh, North Carolina, USA

Pfiesteria piscicida Steidinger & Burkholder is a toxic dinoflagellate that leads to fish and human toxicity. It produces a bioactive substance that leads to cytotoxicity of GH_4C_1 rat pituitary cells. Extracellular adenosine 5′-triphosphate (ATP) acting on $P2X_7$ purinergic receptors induces the formation of a nonselective cation channel, causing elevation of the cytosolic free calcium followed by a characteristic permeabilization of the cell to progressively larger ions and subsequent cell lysis. We investigated whether GH_4C_1 rat pituitary cells express functional $P2X_7$ receptors, and if so, are they activated by a bioactive substance isolated from toxic *P. piscicida* cultures. We tested the selective agonist 2′-3′-*O*-(benzoyl-4-benzoyl)-ATP (BzATP) and antagonists piridoxalphosphate-6-azophenyl-2′-4′-disulfonic acid (PPADS) and oxidized-ATP (oxATP) using elevated cytosolic free calcium in Fura-2 loaded cells, and induced permeability of these cells to the fluorescent dye YO-PRO-1 as end points. We demonstrated that in GH_4C_1 cells, BzATP induces both the elevation of cytosolic free calcium and the permeabilization of the cell membrane. ATP-induced membrane permeabilization was inhibited by PPADS reversibly and by oxATP irreversibly. The putative *Pfiesteria* toxin (pPfTx) also elevated cytosolic free calcium in Fura-2 in GH_4C_1 cells and increased the permeability to YO-PRO-1 in a manner inhibited fully by oxATP. This study indicates that GH_4C_1 cells express a purinoceptor with characteristics consistent with the $P2X_7$ subtype, and that pPfTx mimics the kinetics of cell permeabilization by ATP. *Key words*: GH_4C_1, *Pfiesteria*, purinergic receptors, $P2X_7$, toxin. — *Environ Health Perspect* 109(suppl 5):731–737 (2001). *http://ehpnet1.niehs.nih.gov/docs/2001/suppl-5/731-737melo/abstract.html*

Extracellular adenosine 5′-triphosphate (ATP) acting on purinergic (P2) receptors regulates a variety of functions, using transduction pathways that are dependent on the type of the P2-receptor and on the type of cells where the action occurs (*1,2*). For example, in the nervous system, ATP is co-released with neurotransmitters by exocytosis to modulate the synaptic transmission via the activation of P2X-receptor cation channels (*3*). Macrophages and mast cells express a different functional type of P2X-receptor that changes its ionic selectivity when exposed to extracellular ATP (*4*). In this type of receptor, first designated P2Z and later recognized as $P2X_7$, the formation of a nonselective cation channel is followed by a progressive permeabilization of the cell membrane to ions of larger molecular weight and finally leading to cell lysis (*5*). This distinctive second mode of action involving an apparent increase in pore diameter has been the focus of many studies (*5–10*). P2 receptors have been classified in two different classes: the ionotropic P2X, which forms a nonselective cation channel when activated by an agonist, and the metabotropic G-protein–coupled P2Y (*11*). Structurally, P2X receptors are constituted by the assemblage of subunits, each one with two transmembrane domains (*12,13*), whereas P2Y has the typical structure of a G-protein–coupled receptor with seven membrane-spanning domains (*13*). Seven types of the P2X class of P2 receptors have been cloned ($P2X_1$-$P2X_7$) and are distinguished pharmacologically in two groups on the basis of sensitivity to the ATP congener αβ-ATP. A third group, the $P2X_7$ receptors, is distinguished functionally by ionic conductance (*14*).

The $P2X_7$ activity was first identified in mast cells and macrophages and was suggested to have a role in cytolysis and apoptotic death in cells of the immune system (*15,16*). $P2X_7$ was then cloned from the rat brain (*6*), where it is found in the microglia (*17*). Its presence has been documented in other cell types such as human fibroblasts (*18*) and hepatocytes (*19*), and in the cell lines CHO-K1 (*9*) and GH_4C_1 (*28*). Pharmacological studies identified a characteristic higher affinity of $P2X_7$ to the ATP congener 2′-3′-*O*-(benzoyl-4-benzoyl)-ATP (BzATP) than to ATP itself, and revealed a sensitivity to the ionic environment in the kinetics of cell permeabilization (*21*). The finding that the replacement of extracellular ionic sodium by the larger ion *N*-methyl-D-glucamine (NMDG) facilitates the permeabilization mode of the activated receptor, causing a delay or inhibition of cell lysis (*5*), has been widely used in the functional characterization of the $P2X_7$ (*21*).

It is well known that toxins synthesized by a variety of organisms can selectively bind to ion conduction channels, altering their functional properties and leading to toxicity. The heterotrophic estuarine dinoflagellate *Pfiesteria piscicida* Steidinger & Burkholder was discovered in 1991 by Burkholder and co-workers (*22*) and has been implicated as the causative agent of major fish kills and fish disease in the two largest U.S. mainland estuaries (the Albemarle–Pamlico of North Carolina and Chesapeake Bay in Maryland) (*23*). A second toxic *Pfiesteria* species has subsequently been identified (among a number of organisms morphologically similar to *P. piscicida*, termed "*Pfiesteria*-like" or "*Pfiesteria* look-alike" organisms) from fish-kill/fish-disease events in aquaculture and coastal areas from Delaware to the Gulf of Mexico (*23*). The health hazards attributed to this organism (*24–26*) led to the need to characterize bioactive substances produced by *P. piscicida* capable of causing adverse effects. Research to fully characterize the chemical structure and biological effects of this putative toxin is a current challenge. *P. piscicida* produces a bioactive substance that induces cytotoxicity in GH_4C_1 rat pituitary cells and at nontoxic

This article is based on a presentation at the CDC National Conference on *Pfiesteria*: From Biology to Public Health held 18–20 October 2000 in Stone Mountain, Georgia, USA.

Address correspondence to J.S. Ramsdell, Coastal Research Branch Center for Coastal Environmental Health and Biomolecular Research, NOAA National Ocean Service, 219 Fort Johnson Rd., Charleston, SC 29412 USA. Telephone: (843) 762-8510. Fax: (843) 762-8700. E-mail: john.ramsdell@noaa.gov

The work presented was conducted in partial fulfillment of PhD requirements in Molecular and Cellular Biology and Pathobiology from the Medical University of South Carolina for A.C.M., who was supported in part by a PhD fellowship from Fundação para a Ciência e Tecnologia, Portugal, ref. BD/ 2842/ 93-RN.

This work was funded by the National Oceanic & Atmospheric Administration (NOAA-NOS); and by the North Carolina General Assembly, the Z. Smith Reynolds Foundation, and an anonymous foundation (grants to co-authors Burkholder and Glasgow). The National Ocean Service (NOS) does not approve, recommend, or endorse any proprietary product or material mentioned in this publication. No reference shall be made to NOS, or to this publication furnished by NOS, in any advertising or sales promotion which would indicate or imply that NOS approves, recommends, or endorses any proprietary product or proprietary material mentioned herein or which has as its purpose any intent to cause directly or indirectly the advertised product to be used or purchased because of NOS publication.

Received 8 January 2001; accepted 26 July 2001.

concentrations induces a c-*fos* luciferase reporter gene (*27*). The expression of c-*fos* in neural cells is often associated with elevated cytosolic free calcium $[Ca^{2+}]_i$ (*28*).

Recently we identified the presence of $P2X_7$ receptor expression in GH_4C_1 rat pituitary cells and provided evidence for a role of this receptor type to mediate the action of the putative *Pfiesteria* toxin (pPfTx) in the induction of c-*fos* luciferase (*20*). Here we investigated the ionic properties of the $P2X_7$ receptor in GH_4C_1 cells, and the activation of these characteristic ionic conductances by the pPfTx. We found that GH_4C_1 cells have ionotropic purinergic receptors with pharmacologic and functional properties consistent with the $P2X_7$ subtype and that pPfTx mimics the kinetics of cell permeabilization by ATP.

Material and Methods

Cell Culture

Clonal GH_4C_1 cells were maintained in monolayer cultures in Ham's F10 medium supplemented with 15% horse serum and 2.5% fetal bovine serum ($F10^+$) in a water-saturated atmosphere of 5% CO_2 and 95% air at 37 ± 1°C. Before experiments, cells were harvested from one donor culture dish with 0.02% EDTA and reseeded on glass coverslips at a density of approximately 200,000 cells/cm^2. The cells were grown for 2–5 days, with change of medium each second day. Only cultures with less than 10 passages were used.

Chemicals

Culture medium and sera were purchased from Gibco (Grand Island, NY, USA). ATP, oxidized ATP (oxATP), and BzATP were purchased from Sigma (St. Louis, MO, USA). Piridoxalphosphate-6-azophenyl-2′-4′-disulfonic acid (PPADS) was from Research Biochemical International (Natick, MA, USA). The fluorescent dyes Fura-2/AM, Fura-2 pentapotassium salt and YO-PRO-1 (quinolinium, 4-[(3-methyl-2(3*H*)-benzoxazolylidene) methyl]-1-[3-(triethylammonio)propyl]-, diiodide) were from Molecular Probes (Eugene, OR, USA). Putative toxin was isolated from fish-killing cultures of *P. piscicida* precisely as described (*28*).

Calcium Analysis

GH_4C_1 cells plated in monolayer on glass coverslips were loaded with Fura-2 just before the experiment. Cells were washed twice with Hepes-buffered saline Hanks' balanced salt solution (HBSS)-II (Hepes 20, D-glucose 10, NaCl 118, KCl 4.6, $CaCl_2$ 0.4 mM, pH 7.2) and incubated with 2 µM Fura-2/AM in the same buffered saline in a water-saturated atmosphere of 5% CO_2 at 37 ± 1°C for 30 min. Cells were then washed twice, incubated at room temperature for 20 min, then mounted in a flow-through chamber (FCSII; Bioptechs Inc., Butler, PA, USA). Experiments were performed with an inverted fluorescence microscope [Zeiss 100, oil immersion Zeiss F-Fluor 40× lens (Carl Zeiss, Inc., Thornwood, NY, USA)], using the Attofluor ratio imaging analysis system (Atto Instruments, Rockville, MD, USA). Temperature in the chamber was controlled at 37 ± 1°C and HBSS-II was pumped in a laminar flow over the cells at a constant rate of 100 µL/min. Calcium concentration was calculated by the method of Grynkiewicz (*29*). Excitation wavelengths were 340 and 380 nm, and emission intensity was measured at 510 nm. The cytosolic free calcium concentration in single cells was monitored in real time. At least 30 cells were monitored simultaneously in each experiment. The values of cytosolic free calcium from each cell were averaged after the experiment. We used the *in vitro* method of calibration modified from the Attofluor manual. This method uses two calibration points, a maximum and a minimum correspondent respectively to a saturated calcium solution (10 mM $CaCl_2$) and a solution calcium free (with 10 µM EGTA). One µM Fura-2 pentapotassium was added to each solution, which was used to calibrate the system before each experimental session.

Cell-Permeabilization Analysis

The dye YO-PRO-1, a fluorescent analog of propidium iodide of 629 Da molecular weight, was used to detect cell permeabilization (*5*). GH_4C_1 cells plated in monolayer on glass coverslips were washed twice with HBSS-II and mounted in the flow-through chamber. The experiments were performed using an inverted microscope and the Attofluor imaging system (described for the calcium analysis experiments) but in a single wavelength mode of analysis. A modified Hepes-buffered saline solution, made with NMDG substituting for NaCl (Hepes 20, D-glucose 10, NMDG 118, KCl 4.6, $CaCl_2$ 0.4 mM, pH 7.2) and henceforth designated HBSS-YO, was used in the permeabilization assays (*5*). HBSS-YO was pumped in a laminar flow at the rate of 100 µL/min. Test reagents were diluted in 200 µL HBSS-YO and injected in one of the inflows (see flow-through description below). The flow of the buffered saline was constant throughout the experiments. The excitation wavelength was 460 nm, and emission was measured at 510 nm. At least 30 cells were individually monitored simultaneously in real time during each experiment. Experiments with BzATP were conducted five times, ATP four times, and pPfTx five times. For the experiments where the inhibition by oxATP was tested, cells were preincubated with 300 µM of oxATP in $F10^+$ for 40 min in a water-saturated atmosphere of 5% CO_2 at 37 ± 1°C. Cells were then washed twice and mounted in the flow-through chamber, and the experiments were performed as above.

Flow-Through System

All of our experiments were completed in a closed chamber (FCSII; Bioptechs Inc.) through which a constant laminar flow of the Hepes-buffered saline was maintained over the cells. The inflow was fed by one of two

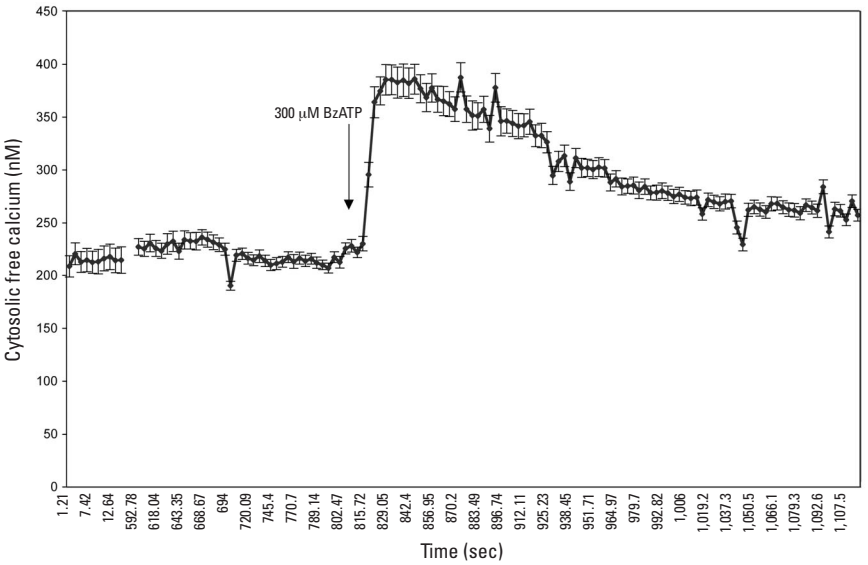

Figure 1. Elevation of the concentration of cytosolic free calcium in the presence of 300 µM BzATP. Cytosolic free calcium concentrations were calculated following the method of Grynkiewicz (*29*), using a K_d of 224 nM Fura-2 for calcium ions. Data are given as the means ± 1 SE of cytosolic free calcium in 30 cells individually monitored simultaneously during a single experiment in real time.

alternate peristaltic pumps that were digitally controlled. A check valve just before the chamber inlet separated the inflows driven from each pump. The test solution was injected into a loop inserted into one of the inflows, and was pumped through the chamber when the respective pump was digitally switched on. Both pumps were set to the flow rate of 100 µL/min. The temperature in the chamber was controlled at 37 ± 1°C.

Data Analysis

Values of light emission from individual cells were averaged and standard errors calculated. One-way analysis of variance was applied to the emission data, corresponding to time points at and just before stimulation by the test substance.

Results

The action of the P2 receptor agonist BzATP on $[Ca^{2+}]_i$ was investigated in GH_4C_1 cells loaded with the fluorescent calcium chelator Fura-2. The baseline $[Ca^{2+}]_i$ was approximately 200 nM and was elevated to a peak of 390 nM within 3–5 sec after exposure to 300 µM BzATP (Figure 1). $[Ca^{2+}]_i$ was maintained above 350 nM in the continuous presence of BzATP and decreased to a plateau of 280 nM when BzATP was washed out.

The permeabilization of the cell membrane to larger ions, a functional characteristic of $P2X_7$ subtype receptors, was next investigated. GH_4C_1 cells were mounted in an inverted microscope under the same conditions of temperature (37 ± 1°C) and flow-through (100 µL/min) used for the first experiment with Fura-2. The dye YO-PRO-1 was present in the flowing solution only at the times indicated in the chart (Figure 2). The background emission was an average of 20 relative fluorescence units [(RFU), used to measure the intensity of light emission] in the absence of the dye and was elevated to less than 25 RFU when the dye was present. The mean emission (n = 30 cells) was nearly 25 RFU in the absence of dye. The mean emission was elevated to less then 40 RFU in the presence of 5 µM YO-PRO-1 and returned to 25 RFU after the dye was washed out. Return of the emission to the initial levels revealed that the fluorescent dye was not trapped in the cells and indicated that the cells were not permeable to the dye. When the dye was delivered simultaneously with BzATP, a gradual but steady increase of emission intensity from the cells reached a level 4-fold higher (96 vs 23 RFU) than the initial emission. The high emission level was maintained after the dye and BzATP were washed out, indicating that the dye had permeated the cells.

Because BzATP caused both a pharmacological and functional action characteristic of $P2X_7$ receptors, we next investigated ATP, the physiologic agonist of the P2 receptors. The mean activity of 60 cells that were monitored simultaneously was determined after normalization by reducing the background level, which also was measured simultaneously (Figure 3). During the periods indicated (Figure 3), the cells were exposed to 5 µM YO-PRO-1 only, or to 5 µM YO-PRO-1 with 200, 400, or 600 µM ATP. There was a concentration-dependent elevation of light emission from the cells, demonstrating that ATP had permeabilized GH_4C_1 cell membranes to the YO-PRO-1 dye A small response (an increase of 2-fold the initial level) was obtained with 200 µM ATP. When the cells were stimulated with 400 or 600 µM ATP, there was a 10-fold increase in activity

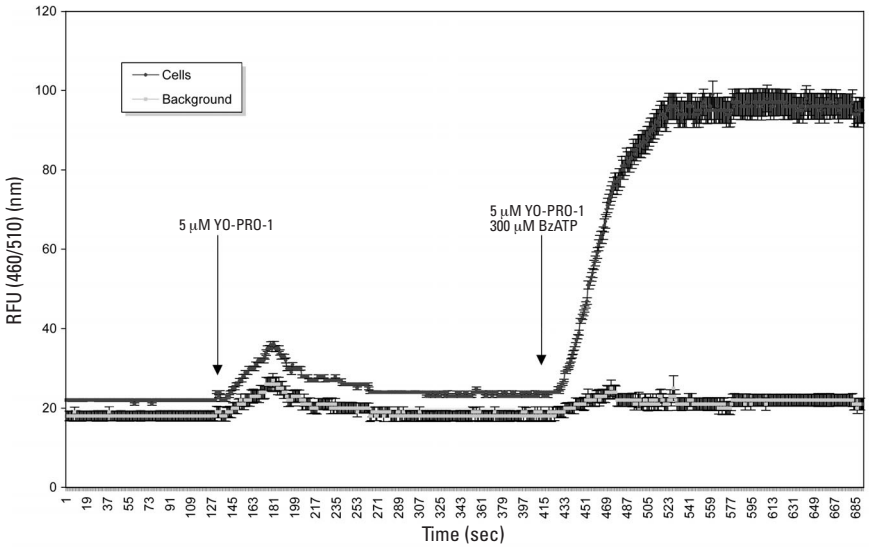

Figure 2. Permeabilization of GH_4C_1 cells to the fluorescent dye YO-PRO-1 in the presence of 300 µM BzATP. Data are given as the mean RFU ± 1 SD from 35 cells collected in a single real-time experiment for the top tracing and as the mean RFU ± 1 SD of the background activity from five selected areas free of cells in the field of view. At the time shown in the chart, 200 µL buffer containing both 300 µM BzATP and 5 µM YO-PRO-1 were being delivered at the same flow rate.

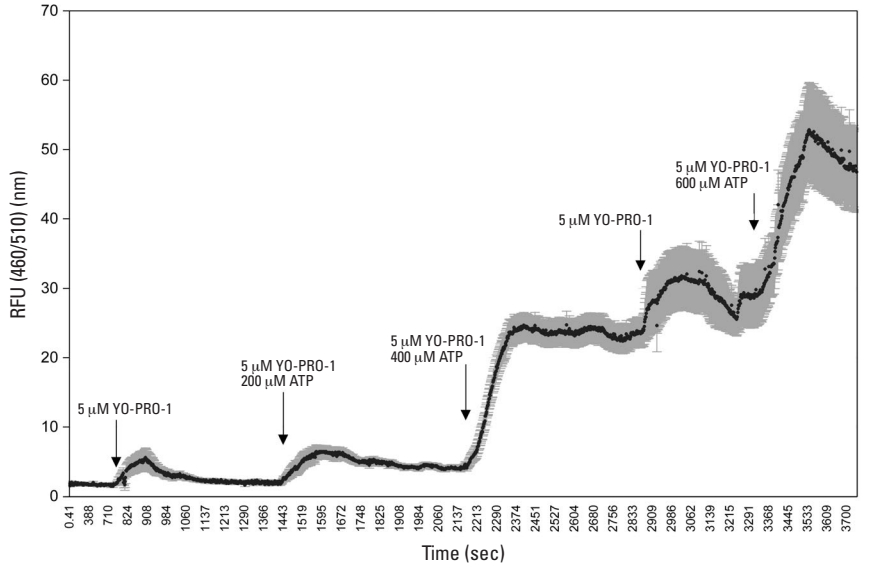

Figure 3. Concentration-dependent permeabilization of GH_4C_1 cells to the fluorescent dye YO-PRO-1 in the presence of ATP (200, 400, and 600 µM). Data are given as the mean RFU ± 1 SD from 30 cells collected in a single real-time experiment, after subtracting the background light intensity, which was monitored simultaneously from 5 selected areas that were free of cells in the field of view. At the time shown in the chart, 200 µL of buffer containing both ATP (200, 400, or 600 µM) and 5 µM YO-PRO-1 were being delivered at the same flow rate.

relative to the level of the emission plateau before each treatment.

To reexamine whether P2 receptors mediate the ATP permeabilization of GH_4C_1, we co-administered PPADS, an antagonist of P2 receptors, and ATP (*13*). GH_4C_1 cells were first treated with 300 mM ATP, leading to accumulation of YO-PRO-1. PPADS given at 300 μM caused a small increase emission, and the addition of 300 μM ATP led to a small increase in dye accumulation. However, this partial inhibitory effect was reversible, and after the antagonist was washed out, led to further accumulation of YO-PRO-1 in the cells (Figure 4). We next investigated the action of oxATP, an irreversible and more selective P2X antagonist (*30,31*) in GH_4C_1 cells. Cells were preincubated with 300 μM oxATP for 30 min in HBSS-II buffered saline, washed twice, and mounted in the flow-through chamber using the Hepes buffer with NMDG substituting NaCl (HBSS-YO), as in the previous experiments. Pretreatment with oxATP fully inhibited the accumulation of YO-PRO-1 in GH_4C_1 cells exposed to 300 and 600 μM ATP (Figure 5).

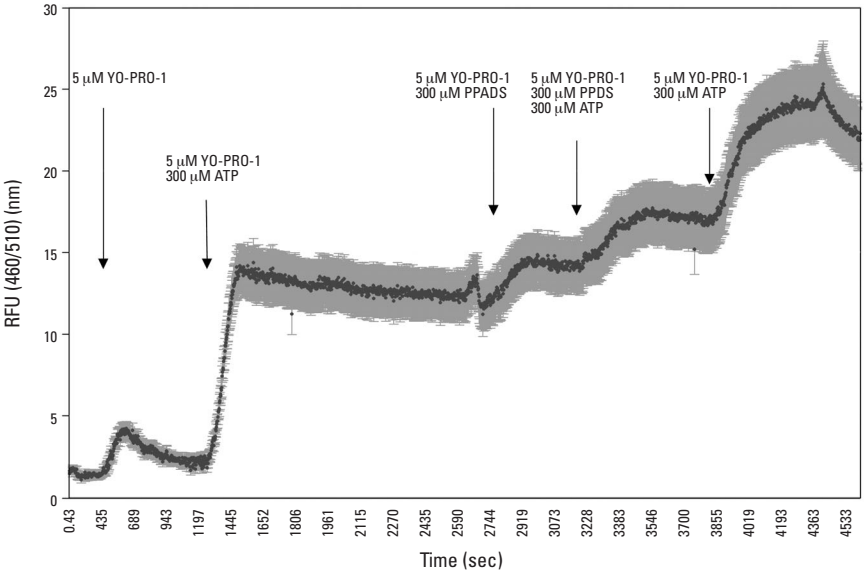

Figure 4. Permeabilization of GH_4C_1 cells to the fluorescent dye YO-PRO-1 by ATP, and its partial inhibition by the purinergic receptor antagonist PPADS. Data are given as the mean RFU ± 1 SD from 30 cells collected in a single real-time experiment after subtracting the background light intensity, which was monitored simultaneously from five selected areas free of cells in the field of view. Test chemicals and concentrations are shown on the chart and were always delivered simultaneously with 5 μM YO-PRO-1 in 200 μL buffer at the same flow rate.

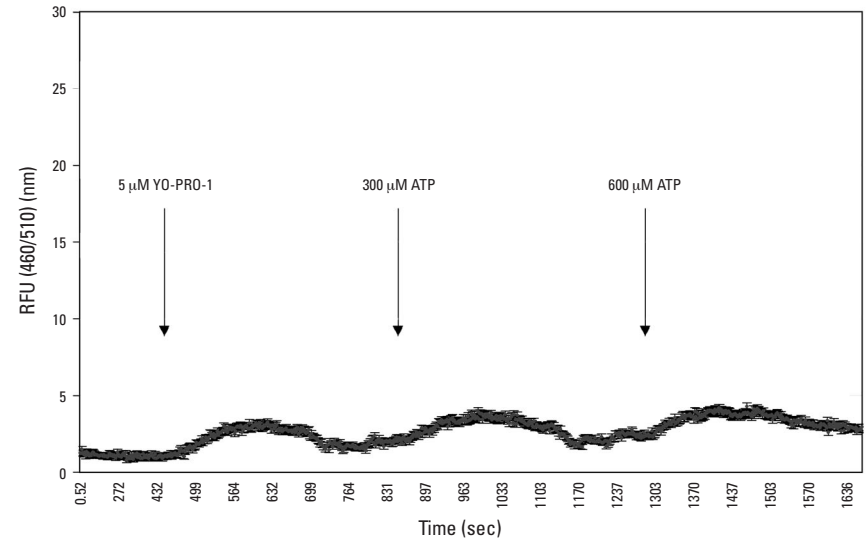

Figure 5. Permeabilization of GH_4C_1 cells to the fluorescent dye YO-PRO-1 by ATP, and its inhibition by 300 μM of the $P2X_7$ antagonist oxATP. Data are given as the mean RFU ± 1 SD from 30 cells individually measured simultaneously in a single real-time experiment after subtracting the background light intensity, which was monitored simultaneously from five selected areas free of cells in the field of view. Test chemicals and concentrations are shown on the chart and were always delivered simultaneously with 5 μM YO-PRO-1 in 200 μL buffer at the same flow rate.

To evaluate the role of $P2X_7$ as a potential target in mediating the toxic effects of *Pfiesteria*, we used a partially purified fraction from a toxic culture of the dinoflagellate. The action of pPfTx on cytosolic free calcium was investigated in GH_4C_1 cells loaded with the fluorescent calcium chelator Fura-2. Cells were mounted on an open coverslip in an inverted fluorescence microscope, and individual cells were monitored under static incubation conditions. With each incremental addition of the pPfTx caused a gradual sustained elevation of $[Ca^{2+}]_i$ that reached near plateau level in about 90 sec (Figure 6). Enhanced effects were observed with further additions, which eventually reached very high values consistent with cytotoxicity. We next examined the effect of the pPfTx on GH_4C_1 cell permeability to YO-PRO-1. Cells were mounted in the flow-through chamber and were exposed to 200 μL of 1 μL/100 μL, 2 μL/100 μL, or 4 μL/100 μL pPfTx. The pPfTx fraction induced the accumulation of YO-PRO-1 in GH_4C_1 cells in a concentration-dependent manner. The intensity of emission was monitored simultaneously in 60 cells (Figure 7). Exposure of the cells to 1 μL/100 μL caused a small elevation of emission from 1 to 5 RFU. Exposure to 2 μL/100 μL was repeated, and in both exposures the average cell emission was elevated with a reproducible effect that doubled the effect produced by exposure to 1 μL/100 μL. Exposure of GH_4C_1 cells to 4 μL/100 μL led to an increase of average cell emission to nearly 58 RFU, an effect 5-fold higher than that observed from exposure to 2 μL/100 μL (Figure 7). When we used GH_4C_1 cells that previously had been incubated with 300 mM oxATP, the accumulation of YO-PRO-1 in GH_4C_1 cells exposed to 4 μL/100 μL pPfTx was inhibited (Figure 8). Further exposure to 400 μM ATP also failed to induce the accumulation of dye in these cells.

Discussion

This research provides evidence for a P2 receptor with the functional characteristics of the $P2X_7$ type in GH_4C_1 cells. We used two signal transduction measurements to identify this receptor. One was the ability of the selective agonist BzATP to elevate the cytosolic free calcium. The other was the subsequent accumulation of the fluorescent dye YO-PRO-1 due to the permeabilization of the cells to larger ions. In GH_4C_1 cells, BzATP

induced a rapid calcium response that elevated cytosolic free calcium 2-fold. After the agonist was washed out, the effect persisted for at least 3 min. When GH_4C_1 cells were exposed to BzATP in the presence of the fluorescent dye YO-PRO-1, a gradual accumulation of the dye in the cells was observed. The comparison between the effect of BzATP on the concentration of cytosolic calcium, and on the accumulation of YO-PRO-1 in the cells, corresponds to the dynamics of pore formation characteristic of the purinoceptor $P2X_7$ (*8,12,18*). Once activated by an agonist, $P2X_7$ forms a nonselective cation channel, a characteristic of the ionotropic P2X class of P2 receptors. The influx of calcium ions causes the elevation of the cytosolic free calcium. $P2X_7$ differs from the other members of P2X receptors in that its activation leads to the cell membrane permeability to larger ions (*6*). This characteristic has been studied using fluorescent dyes, particularly YO-PRO-1 (a derivative of propidium iodide), which are ions of large molecular weight with affinity to nucleic acids (*5*). The sensitivity to the selective agonist BzATP and the accumulation of YO-PRO-1 in GH_4C_1 cells provides evidence for the presence in these cells of an ionotropic purinoceptor with the functional characteristics of $P2X_7$.

To further characterize the induction of cell permeability in GH_4C_1 cells by the activation of P2 receptors, we exposed cells to increasing concentrations of ATP. We observed that ATP induces the permeability of GH_4C_1 cells to YO-PRO-1 in a concentration-dependent manner. The reversibility of the ATP-induced permeability of the cells was also shown in this experiment, as the cells did not accumulate YO-PRO-1 when they were exposed to the dye both in the absence of ATP and after observed induction by 400 µM of the agonist. We next used two classes of antagonists of P2 receptors to inhibit the accumulation of YO-PRO-1 in GH_4C_1 cells in response to ATP: PPADS, a reversible antagonist of P2 receptors, and oxATP, a selective and irreversible inhibitor of $P2X_7$ (*6*). PPADS partially inhibited cell permeability to YO-PRO-1 by ATP, and this partial inhibition was reversed after the antagonist was washed out. To investigate the effect of the $P2X_7$ selective antagonist oxATP, we pretreated cells with the antagonist (*30,31*). Pretreatment of GH_4C_1 cells with oxATP fully inhibited the accumulation of YO-PRO-1 during exposure to 300 and 600 µM ATP. The ability of a selective antagonist to prevent the accumulation of YO-PRO-1 provided a second line of evidence for functional $P2X_7$ receptors in GH_4C_1 cells.

We next investigated the role of the receptor functionally characterized in this work as a potential target for the toxicity of the dinoflagellate *Pfiesteria*. A bioactive substance has been identified in toxic *Pfiesteria* cultures with cytotoxic selectivity to GH_4C_1 cells based upon a panel of different cell types (*27*). We report here that the pPfTx elevates cytosolic free calcium in Fura2-loaded GH_4C_1 cells. The elevation of calcium is sustained and is consistent with activation of a membrane channel that gates calcium. The time course of elevated cytosolic free calcium is consistent with activation of $P2X_7$ receptors (*32*). Calcium is a second messenger, and one of its downstream signaling events is among those factors that induce the immediate response gene c-*fos*. For that reason, the sustained elevation of cytosolic free calcium by pPfTx is consistent with the induction of the c-*fos*

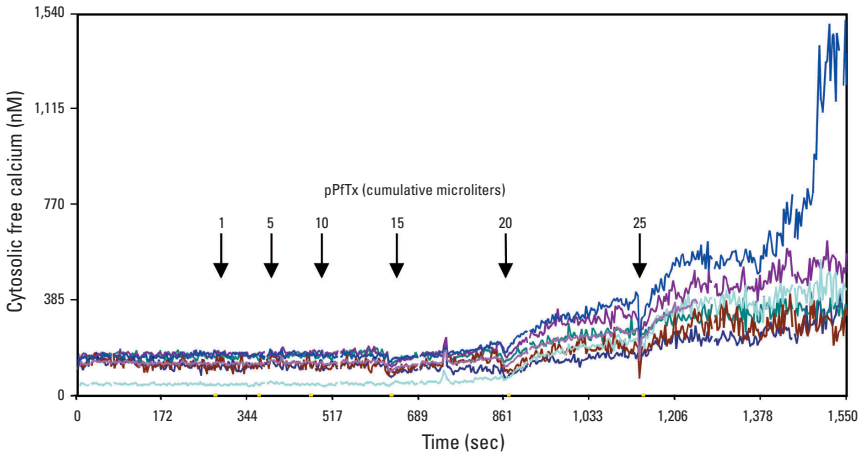

Figure 6. Elevation of the concentration of cytosolic free calcium in the presence of putative *Pfiesteria* toxin pPfTx. Cytosolic free calcium concentrations were calculated following the method of Grynkiewicz (*29*), using a K_d of 224 nM Fura-2 for calcium ions. GH_4C_1 cells loaded with Fura-2 were treated with increasing amounts of pPfTx, and the concentration of free cytosolic calcium was monitored individually in 7 cells in real time. Data are given as the activities (RFU) from individual cells measured simultaneously in an experiment repeated 4 times with similar results. The pPfTx is expressed as microliters of an assay-guided fraction of a methanol/water extract of toxic *Pfiesteria* culture medium. Exposure of the cells to 15 µL pPfTx led to an increase of cytosolic free calcium, which was enhanced in a dose-dependent manner by further additions of 5 µL each.

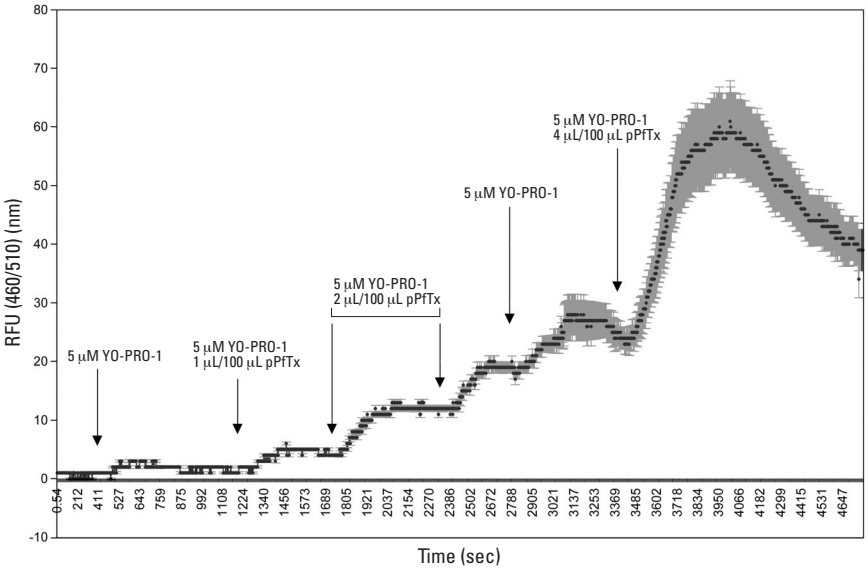

Figure 7. Concentration-dependent permeabilization of GH_4C_1 cells to the fluorescent dye YO-PRO-1 in the presence of pPfTx. Data are given as the mean RFU ± 1 SD from 60 cells that were individually measured simultaneously in a single real-time experiment after subtracting the background light intensity, which was also monitored simultaneously from five selected areas free of cells in the field of view. The pPfTx was always delivered simultaneously with 5 µM YO-PRO-1 in 200 µL buffer at the same flow rate. Where indicated, only the dye (without pPfTx) was delivered in the same manner.

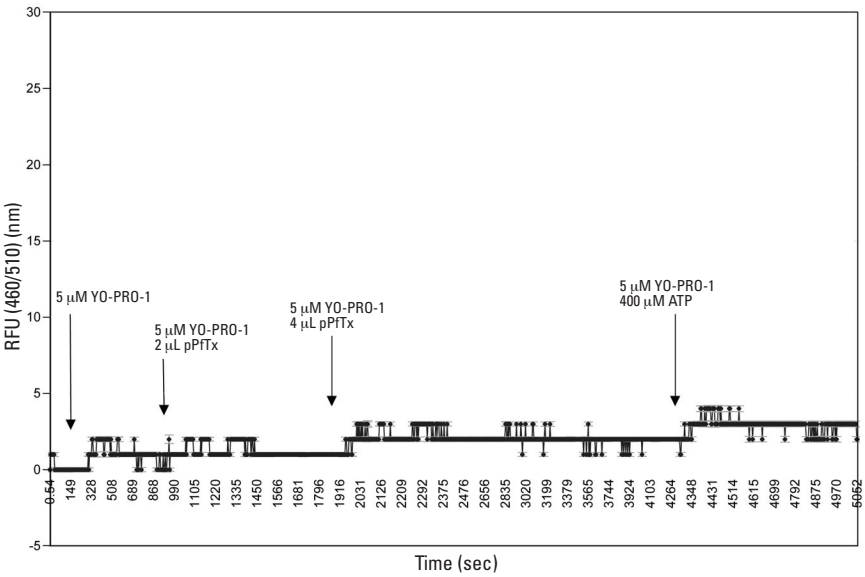

Figure 8. Permeabilization of GH_4C_1 cells by the pPfTx to the fluorescent dye YO-PRO-1 and its inhibition by oxATP, which is a specific antagonist of the $P2X_7$ purinergic receptor. Data are given as the mean RFU ± 1 SD of the activity from 60 cells individually measured simultaneously in a single real-time experiment, after subtracting the background light intensity which was also monitored simultaneously from five selected areas free of cells in the field of view. We used 400 μM ATP as a positive control. Test chemicals were always delivered simultaneously with 5 μM YO-PRO-1 in 200 μL buffer at the same flow rate.

luciferase construct in GH_4C_1 cells, a downstream response used to originally identify the action of this substance (*20,27*). Activation of $P2X_7$ receptors leads to strong induction of additional transcription factors as well, including nuclear factor (NF)-kappaB and the nuclear factor of activated T cells (NFAT), both of which are associated with cytokine production (*33*). NFAT is induced rapidly and requires the entry of extracellular calcium. NFAT has a unique DNA binding region, yet binds cooperatively with the Fos/Jun heterodimer to the regulation region of the interleukin-2 gene (*34*). By contrast, NF-kappaB is induced more slowly and may require more downstream signaling events (*35*). Subsequent to elevating cytosolic free calcium, pPfTx induced the permeabilization of GH_4C_1 cells to YO-PRO-1. This action of pPfTx is consistent with its cytotoxic effect (*27*) and the decreased c-*fos* luciferase activity (*20*). The permeabilizing effect of pPfTx in GH_4C_1 cells was completely inhibited by oxATP. These results provide an additional line of evidence that the previously described cytotoxic effect of pPfTx (*27*) likely is mediated by $P2X_7$ receptors (*20*).

Defining the role for P2 receptors has been hampered partly because few, if any, natural specific agonists have been identified for purinergic receptors. One toxin that also shows a strong cytotoxic response in GH_4C_1 and other cell types is maitotoxin (*36,37*). Although the primary target for maitotoxin has not been identified, it does elevate cytosolic calcium in GH_4C_1 cells by activating a calcium-dependent membrane depolarization (*38,39*), one that appears to involve chloride conductances (*40*). Maitotoxin induces c-*fos* luciferase and at higher concentrations cytotoxicity in GH_4C_1 cells expressing this construct (*41*). Maitotoxin has been found to activate a cytolytic pore in several other cell types; however, overexpressing $P2X_7$ receptors in HEK-292 cells, which leads to substantial BzATP responses, fails to enhance the response to maitotoxin (*42,43*). These results indicate that $P2X_7$ is not a primary target for maitotoxin, although activation of a cytolytic pore is a likely downstream response. Thus pPfTx may prove to be a unique pharmacological probe for P2 receptors. More definitive characterization of pPfTx will require larger-scale production of toxic *Pfiesteria* for structural resolution of the toxin.

A role of $P2X_7$ receptors in the action of Pfiestera toxin is of interest, considering that this toxic dinoflagellate has been reported to cause a range of health impacts in both finfish and humans (*22–26*). The effects linked to *Pfiesteria* toxicity may be related to an inflammatory response, either in macrophages in the periphery or microglia in brain tissue. Implication of $P2X_7$ receptors as a potential target for the bioactive substance produced by toxic *P. piscicida* provides a common basis for the investigation of symptoms that previously have been regarded as unrelated, such as ulcers in menhaden and cognitive dysfunction in humans.

References and Notes

1. Burnstock G. Development and perspectives of the purinoceptor concept. J Auton Pharmacol 16:295–302 (1996).
2. Surprenant A. Functional properties of native and cloned P2X receptors. Ciba Found Symp 198:208–222 (1996).
3. Khakh BS, Bao XR, Labarca C, Lester HA. Neuronal P2X transmitter-gated cation channels change their ion selectivity in seconds. Nat Neurosci 2:322–330 (1999).
4. Steinberg TH, Newman AS, Swanson JA, Silverstein SC. ATP^{4-} permeabilizes the plasma membrane of mouse macrophages to fluorescent dyes. J Biol Chem 262:8884–8888 (1987).
5. Virginio C, MacKenzie A, North AR, Surprenant A. Kinetics of cell lysis, dye uptake and permeability changes in cells expressing the rat $P2X_7$ receptor. J Physiol 519:335–346 (1999).
6. Surprenant A, Rassendren F, Kawashima E, North AR, Buell G. The cytolytic P_{2Z} receptor for extracellular ATP identified as a P2X receptor ($P2X_7$). Science 272:735–738 (1996).
7. Rassendren F, Buell GN, Virginio C, Collo G, North AR, Surprenant A. The permeabilizing ATP receptor, $P2X_7$. J Biol Chem 272:5482–5486 (1997).
8. Virginio C, Church D, North RA, Surprenant A. Effects of divalent cations, protons and calmidazolium at the rat $P2X_7$ receptor. Neuropharmacology 36:1285–1294 (1997).
9. Michel AD, Chessell IP, Hibell AD, Simon J, Humphrey PPA. Identification and characterization of an endogenous $P2X_7$ (P2Z) receptor in CHO-K1 cells. Br J Pharmacol 125:1194–1201 (1998).
10. Coutinho-Silva R, Persechini PM, Bisaggio RD, Perfettini JL, Neto AC, Kanellopoulos JM, Motta-Ly I, Dautry-Varsat A, Ojcius DM. P2Z/ $P2X_7$ receptor-dependent apoptosis of dendritic cells. Am J Physiol 276(5 Pt 1):c1139–c1147 (1999).
11. Burnstock G. P2 purinoceptors: historical perspective and classification. Ciba Found Symp 198:1–28 (1996).
12. Bianchi BR, Lynch KJ, Touma E, Niforatos W, Burgard EC, Alexander KM, Park HS, Yu H, Metzger R, Kowaluk E, et al. Pharmacological characterization of recombinant human and rat P2X receptor subtypes. Eur J Pharmacol 376:127–138 (1999).
13. Ralevic V, Burnstock G. Receptors for purines and pyrimidines. Pharmacol Rev 50:413–478 (1998).
14. MacKenzie AB, Surprenant A, North AR. Functional and molecular diversity of purinergic ion channel receptors. Ann N Y Acad Sci 868:716–729 (1999).
15. Buisman HP, Steinberg TH, Fischbarg J, Silverstein SC, Vogelzang SA, Ince C, Ypey DL, Leigh PC. Extracellular ATP induces a large nonselective conductance in macrophage plasma membranes. Proc Natl Acad Sci U S A 85:7988–7992 (1988).
16. Nuttle LC, Dubyak GR. Differential activation of cation channels and non-selective pores by macrophage P2Z purinergic receptors express in Xenopus oocytes. J Biol Chem 269:13988–13996 (1994).
17. Ferrari D, Chiozzi P, Falzoni S, Susino MD, Collo G, Buell G, Virgilio FD. ATP-mediated cytotoxicity in microglial cells. Neuropharmacology 36:1295–1301 (1997).
18. Solini A, Chiozzi P, Morelli A, Fellin R, Virgilio FD. Human primary fibroblasts in vitro express a purinergic $P2X_7$ receptor coupled to ion fluxes, microvesicle formation and IL-6 release. J Cell Sci 112:297–305 (1999).
19. Zoeteweij JP, vande Water B, DeBont HJGM, Nagelkerke JF. The role of a purinergic P2Z receptor in calcium-dependent cell killing of isolated rat hepatocytes by extracellular adenosine triphosphate. Hepatology 23:858–865 (1996).
20. Kimm-Brinson KL, Moeller PDR, Barbier M, Glasgow HB Jr, Burkholder JM, Ramsdell JS. Identification of a $P2X_7$ receptor in GH_4C_1 rat pituitary cells: a target for a bioactive substance produced by *Pfiesteria piscicida*. Environ Health Perspect 109 (5):457–462 (2001).
21. Michel AD, Chessel IP, Humphrey PPA. Ionic effects on human recombinant $P2X_7$ receptor function. Naunyn-Schmiedebergs Arch Pharmakol 359:102–109 (1999).
22. Burkholder JM, Noga EJ, Hobbs CW, Glasgow HB, Smith SA. New "phantom" dinoflagellate is the causative agent of major estuarine fish kills. Nature 358:407–410 (1992).
23. Burkholder JM, Glasgow HB Jr. Trophic controls on stage transformation of a toxic ambush-predator dinoflagellate. J Eukaryot Microbiol 44:200–205 (1997).
24. Glasgow HB Jr, Burkholder JM, Schemechel DE, Tester PA, Rublee PA. Insidious effects of a toxic estuarine dinoflagellate on fish survival and human health. J Toxicol Environ Health 46:501–522 (1995).
25. Burkholder JM. Implications of harmful algal marine microalgae and heterotrophic dinoflagellates in management of sustainable marine fisheries. Ecol Appl (suppl 8):S37–S62 (1998).

26. Grattan LM, Oldach D, Perl TM, Lowitt MH, Matuszak DL, Dickson C, Parrot C, Shoemaker RC, Kauffman CL, Wasserman MP, et al. Learning and memory difficulties after environmental exposure to waterways containing toxin-producing *Pfiesteria* or *Pfiesteria*-like dinoflagellates. Lancet 352:532–539 (1998).
27. Fairey ER, Edmunds JSG, Deamer-Melia NJ, Glasgow HB Jr, Johnson FM, Moeller PR, Burkholder JM, Ramsdell JS. Reporter gene assay for fish-killing activity produced by *Pfiesteria piscicida*. Environ Health Perspect 107:711–714 (1999).
28. Sonnenberg JL, Mitchelmore C, MacGregor PF, Hempstead J, Morgan JI, Curran T. Glutamate receptor agonists increase the expression of Fos, FRA, and AP-1 DNA binding activity in the mammalian brain. J Neurosci Res 24:72–80 (1989).
29. Grynkiewicz G, Poenie M, Tsien RY. A new generation of Ca^{++} indicators with greatly improved fluorescence properties. J Biol Chem 260:3440–3450 (1985).
30. Murgia M, Hanau S, Pizzo P, Rippa M, Di Virgilio F. Oxidized ATP: an irreversible inhibitor of the macrophage purinergic P2Z receptor. J Biol Chem 268:8199–8203 (1993).
31. Grahames CBA, Michel AD, Chessel IP, Humphrey PPA. Pharmacological characterization of ATP- and LPS-induced IL-1β release in human monocytes. Br J Pharmacol 127:1915–1921 (1999).
32. Ross PE, Ehring GR, Cahalan MD. Dynamics of ATP-induced calcium signaling in single mouse thymocytes. J Cell Biol 138:987–998 (1997).
33. Ferrari D, Stroh C, Schulze Osthoff K. $P2X_7$ purinoreceptor-mediated activation of transcription factor NFAT in microglial cells. J Biol Chem 274:13205–13210 (1999).
34. Chen L, Glover JNM, Hogan PG, Rao A, Harrison SC. Structure of the DNA-binding domains of NFAT, Fos and Jun bound to DNA. Nature 392:42–48 (1998).
35. Ferrari D, Wesselborg S, Bauer MKA, Schulze Osthoff K. Extracellular ATP activates transcription factor NF-kappaB through the P2Z purinoreceptor targeting NF-kappaB p65 (RelA). J Cell Biol 139:1635–1643 (1997).
36. Gusovsky F, Daly JW. Maitotoxin: a unique pharmacological tool for research on calcium-dependent mechanism. Biochem Pharmacol 39:1633–1639 (1990).
37. Xi D. Mechanisms of Maitotoxin and Domoic Acid Action to Elevate Cytosolic Free Calcium [PhD Thesis]. Charleston, SC:Medical University of South Carolina, 1996.
38. Xi D, Van Dolah FM, Ramsdell JS. Maitotoxin activates type L-voltage dependent calcium channels and induces a calcium-dependent membrane depolarization in GH_4C_1 pituitary cells. J Biol Chem 267:25025–25031 (1992).
39. Xi D, Kurtz DR, Ramsdell JS. Maitotoxin induces calcium entry by nimodipine sensitive and insensitive pathways in GH_4C_1 pituitary cells. Biochem Pharmacol 166:49–56 (1996).
40. Young RC, McLaren M, Ramsdell JS. Maitotoxin increases voltage independent chloride currents in GH_4C_1 pituitary cells. Nat Toxins 3:419–427 (1995).
41. Fairey ER, Ramsdell JS. Reporter gene assays for algal-derived toxins. Nat Toxins 7:415–421 (1999).
42. Schilling WP, Sinkins WG, Estacion M. Maitotoxin activates a nonselective cation channels and a P2Z/ $P2X_7$-like cytolytic pore in human skin fibroblasts. Am J Physiol 275:C755–C765 (1999).
43. Schilling WP, Wasylyna T, Dubyak GR, Humphreys BD, Sinkins WG. Maitotoxin and P2Z/ $P2X_7$ purinergic receptor stimulation activate a common cytolytic pore. Am J Physiol 275: C766–C776 (1999).